

LOW MASS DENSITY WIDE FIELD FAR-IR/SUBMILLIMETER TELESCOPE SYSTEMS

M. DRAGOVAN^{1,2}

Draft version October 29, 2018

ABSTRACT

Fundamentally new technology is described for constructing low areal mass density ($\sim 1\text{kg/m}^2$), high precision ($< \sim 10\mu\text{m}$ RMS) reflectors scalable to large apertures (~ 10 to 20 meters) for use as the primary element of a telescope system. A large reduction in mass is achieved by minimizing the mass of the reflective surface using a high reflectivity metallic membrane. A wide field diffraction limited telescope system can be constructed using the primary reflector in conjunction with secondary and tertiary optics.

Subject headings: instrumentation: telescopes

1. INTRODUCTION

Progress in observational astrophysics parallels the development of telescope technology and the associated instrumentation. The problem of constructing telescopes using polished metal mirrors has a long history tracing back to Gregory(1663), Newton(1672), and Cassegrain. The first successful mirrors with silver reflecting surfaces on a glass substrate were constructed in the late 1850's by von Steinheil and Foucault (King 1979). Current state-of-the-art reflectors can trace their roots back to this technology.

The function of the substrate is to support the thin layer of high reflectivity material; the glass or metal substrate is formable into a shape that has useful optical properties. In current state-of-the-art telescopes the mass of the substrate is $10^3 - 10^6$ times the mass of the reflecting layer. Clearly, new perspectives on telescope systems are necessary to reduce the cost and mass of the primary element.

The technology described in this *letter* achieves a significant reduction in mass by minimizing the thickness of the substrate. The telescope systems described use reflectors whose three dimensional shapes and curvatures are formed by the bending or stretching of a membrane over an appropriate boundary. The membrane is deformed by this process, with the result that the surface assumes a shape that concentrates electromagnetic radiation. If the field of view needs to be larger than can be afforded by a single primary reflector, subsequent optics can correct the aberrations intrinsic to the primary. In either case, a diffraction limited system will result. By using suitable materials for the membrane and other structures, systems with very low areal mass density ($\sim 1\text{kg/m}^2$) that are scalable to large apertures (~ 10 to 20 meters) are constructable.

A number of designs for two and three mirror systems have been developed, resulting in systems that have large focal surfaces (Schroeder 1987). The systems described are generally on-axis, where the secondary and tertiary optics obstruct the primary reflector. Scattering and diffraction of the incident electromagnetic radiation by the secondary optics and its support structure reduces the performance of the overall system. This is particularly problematic for observations of low-contrast objects, or in communications systems where cross-talk between nearby antennas is un-

desirable.

The solution is to use an unobstructed, off-axis design. Unfortunately, the field-of-view of such a system is limited unless steps are taken to control the new set of off-axis aberrations. A solution using confocal conic reflectors was devised by Dragone (1982). Other designs, such as the aplanatic Gregorian or the Schwarzschild (1905; Claydon 1975) solution have lower distortion and provide a wider field-of-view for off-axis systems at the expense of greater complexity of the surface shapes.

A wide field-of-view off-axis three element design is discussed, in which the secondary forms an image of the primary on a third reflector. The combination of the secondary and tertiary gives a wide field and also corrects for aberrations and defects intrinsic to the primary reflector.

2. AREAL DENSITY

Current technology millimetric telescopes have densities of order 10kg/m^2 , a factor of $\sim 10^3$ between the mass of the reflecting layer and that of the support structure. For optical telescopes the situation is much worse where the current state-of-the art has density of order 150kg/m^2 , the supporting substrate $\sim 10^6$ times more massive than the reflecting layer.

The areal density of the reflecting layer is given by $\sigma_r = \rho_r t$ with t the thickness of the reflecting layer, and ρ_r the density. The thickness of the reflecting layer of a high electrical conductivity metallic film can be determined, to good approximation for a specific reflecting material, by considering the skin depth

$$\delta = 1/\sqrt{\pi c \mu \sigma_e / \lambda},$$

where σ_e is the conductivity of the reflecting surface, λ is the wavelength, and $\mu = 400\pi\text{nH/m}$. With a thickness of $t = 7\delta$, the surface is opaque and the wave is reflected with low loss. For a very good conductor such as copper $\sigma_e = 5.7 \times 10^7(\Omega\text{m})^{-1}$. In the case of optical light ($\lambda = 0.5\mu\text{m}$) the film only has to be $\sim 50\text{nm}$ thick to reflect the incident light; for millimeterwaves ($\lambda = 1000\mu\text{m}$) a $\sim 1\mu\text{m}$ thickness is required. This gives an areal density $\sigma_r \sim 8 \times 10^{-3}\text{kg/m}^2$ in distinct contrast to the areal density of the substrate material, which can be many orders of magnitude greater.

¹Enrico Fermi Institute, University of Chicago, Chicago, IL 60637, mrk@oddjob.uchicago.edu

²Jet Propulsion Laboratory, California Institute of Technology, Pasadena, CA 91125

By examining existing telescopes one finds that the areal mass density of the supporting substrate (generally some form of glass) is $\sigma \propto d^{0.5}$, where d is the aperture diameter. This is independent of the technology used, or the epoch when the telescope was constructed. In comparison, the areal density of a membrane reflector system scales differently, and is straightforward to calculate. For the reflective membrane

$$\sigma_r = \rho_r t_r.$$

For the supporting boundary

$$\sigma_b = 4\rho_b h(d)\Delta d/d$$

where $h(d)$ is the functional dependence of the boundary thickness with diameter, and Δd is the width of the boundary. The total density is simply the sum

$$\sigma = \sigma_r + \sigma_b = \rho_r t_r + 4\rho_b h(d)\Delta d/d.$$

It is instructive to note two cases, $h(d) = h$ (a constant height ring), and $h(d) = h_o(d/d_o)^{1/3}$ (a constant stiffness ring). In both cases the areal density decreases with aperture. Only if the ring has $h(d) = h_o(d/d_o)^\alpha$ with $\alpha > 1$ does σ grow with d ,

$$\sigma = \rho_r t_r + 4\rho_b (h_o/d_o) (d/d_o)^{\alpha-1} \Delta d.$$

This is in distinct contrast to the scaling relationship for existing telescopes, $\sigma \propto d^{0.5}$. Thus, not only is a membrane reflector less massive to begin with, but the areal density can actually *decrease* with larger apertures if the ring and membrane are appropriately chosen. Clearly, the areal density of a telescope system can be reduced by orders of magnitude if the relatively massive supporting substrate can be minimized while maintaining the desired reflective surface.

3. MEMBRANE SURFACES

Deformable surfaces are naturally categorized by their Gaussian curvature, an intrinsic property of any surface. All surfaces can be broadly categorized as 1) those that have zero Gaussian curvature, and 2) all others. As is well known from differential geometry the Gaussian curvature is given by $K = \kappa_1 \kappa_2$, where κ_1 and κ_2 are the principal curvatures at a given point on the surface. Membrane surfaces with both zero and non-zero Gaussian curvature can be constructed and are considered in turn.

3.1. Category 1: $K = 0$

A surface with zero Gaussian curvature is either flat or has the shape of a trough, so that one of the principal curvatures is always zero. Such a surface can be formed by bending along only one axis. If the shape of the surface in the curved direction is a parabola, then a line focus results for an incident plane wave. To produce a point focus, a system of two trough-shaped reflectors properly oriented with respect to each other must be used. A perspective view of such a system is presented in Fig 1.

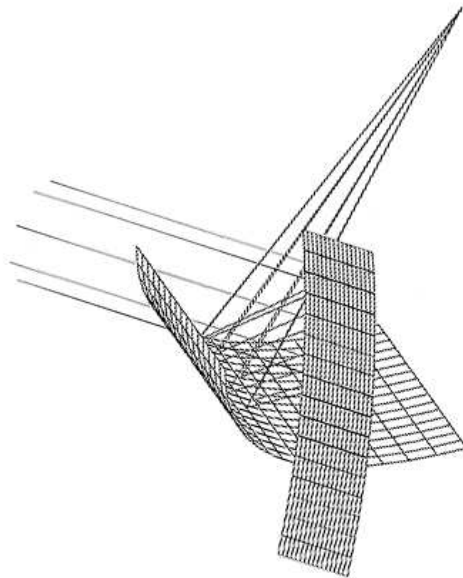


FIG. 1.— The layout of a two mirror reflector system where the individual reflectors are parabolic cylinders. The orientation and curvatures of the individual reflectors are chosen so that a point focus results for an incident plane wave. The reflectors as illustrated are greatly oversized to emphasize the curvatures of each reflective element. It is clear by inspection that the system is completely unobstructed.

In order for this system to focus and have a completely unobstructed aperture the focal lengths of the two individual reflectors must be unequal. The aberrations of the system are identical to those of an off-axis paraboloid with focal length f_1 in the direction which the first reflector focuses, and f_2 in the orthogonal direction, with the subscripts referring to the first or second reflector. For the specific system displayed in figure 1, the extent of the focal surface is 30×30 diffraction limited pixels independent of wavelength. The Airy disk is not circular, but has eccentricity

$$e = (1 - (f_2/f_1)^2)^{1/2}.$$

The parabolic-cylindrical surfaces are formed by tensioning a reflective foil over a frame which has a parabolic contour along one axis and is rigid enough to support the tensioning. The alignment of the two reflectors is critical to the performance of the system. An arrangement of six adjustable rigid struts connecting the two reflectors completely constrains all degrees of freedom while allowing the adjustment of the relative orientation of the two reflectors (Stewart 1965).

3.2. Category 2: $K \neq 0$

Surfaces with non-zero Gaussian curvature can only be formed by stretching or deforming a membrane along both axes. The shape and curvature the surface assumes depends sensitively upon the boundary over which the membrane is stretched, the pressure, and the mechanical material properties of the membrane. If the boundary is circular an axisymmetric reflector results. However, the boundary need not be circular, nor planar; the only requirement is that it is described by a space curve that closes upon itself. The surface constructed has the useful optical property that it can concentrate electromagnetic radiation.

If the elastic limit of the material composing the membrane is exceeded, the deformation is permanent and the

pressure may be released resulting in a self supporting reflector. If the elastic limit is not exceeded, a means of maintaining tension in the membrane is necessary to hold the membrane in the stretched state. The tensioning of the membrane is accomplished by keeping a constant pressure differential on the surface. This results in a membrane structure that has uniform or continuous support over the entire surface.

4. PLASTICALLY DEFORMED MEMBRANES

A pressurized membrane takes on a shape that minimizes the total energy of the system consisting of the membrane, the gas and the structure rigidly holding the membrane. There are three distinct shapes that can form, depending upon how the surface tension, γ , in the membrane distributes itself. Soap films, elastically deformed membranes, and plastically deformed membranes are discussed.

4.1. Modeling the membrane's shape

Soap films take on shapes that minimize the energy of the film. Since the energy of the film is proportional to the surface area, the question of finding the minimal energy surface reduces to finding the surface of minimal area satisfying the boundary conditions. The problem of finding minimal surfaces is known as Plateau's problem, after the Belgian physicist who studied the problem using soap films (Almgren 1969; Isenberg 1992). An unpressurized soap film is a minimal surface and has zero mean curvature $H = (\kappa_1 + \kappa_2)/2 = 0$. A pressurized soap film has non-zero constant mean curvature ($H \neq 0$).

By choosing the appropriate curve for the boundary and pressurizing the film so that it bulges out from the frame, convex or concave surfaces can be formed. In the simplest incarnation the boundary can be chosen so that the film is a segment of a torus, with the degenerate case being a circular boundary which yields a spherical surface. This is both interesting and useful because a segment of any surface with non-zero mean curvature can be approximated to some degree by a toroidal segment (a surface that has two radii of curvature). An off-axis segment of an ellipse or parabola can be fit quite well by a toroidal segment (Cardona-Nunez et al. 1987).

The soap film is the special case of a membrane where the material can redistribute itself so that the tension γ is everywhere constant. Next is a rigid membrane that remains elastic, but has considerable deformation. Here $\gamma(r, \theta)$, is *not* constant as can easily be seen by noting that the at the boundary, where the membrane is clamped, the tension is fixed; however, in the free radial direction the tension can change (i.e. $\gamma(r, \theta) = \gamma(r)$). The third case is that of plastic deformation. Again $\gamma(r, \theta)$ is not constant, but when the pressure is released, the membrane *does not* return to its original state. This is the situation of the membrane reflectors. A variational analysis can be performed for the elastic and plastic flow cases (Murphy 1987; Weil and Newmark 1955), with the result that the shape of the membrane is well approximated as a conic section with higher order polynomial deviations.

The model used to predict the shape of the deformed surface is that of the soap bubble, where the metallic membrane has been sufficiently deformed so that this is a good approximation. The governing equation for the surface

$u(x, y)$ is

$$\nabla \cdot \left(\frac{\nabla u}{\sqrt{1 + |\nabla u|^2}} \right) = p/2\gamma = \left(\frac{1}{r_1} + \frac{1}{r_2} \right),$$

where r_1 and r_2 are the two radii of curvature of the surface, and p is the pressure difference between the inside and outside of the membrane (Bateman 1932; Struik 1961). This non-linear equation may be solved numerically given the geometrical boundary, the pressure, and the surface tension.

4.2. Fabrication and Characterization

A rigid volume is capped with a thin, flat, reflective, and stretchable material (the membrane). The volume is pressurized with a gas, similar to inflating a balloon or soap bubble. The resulting membrane surface is analytically represented by a conic section with polynomial correction terms.

The surface profile of a free standing plastically deformed membrane was measured using a non-contacting laser displacement sensor. The data were fit to a parabola in order to evaluate the magnitude of the wavefront error that needs to be corrected. The residuals of the fit are plotted in fig 2.

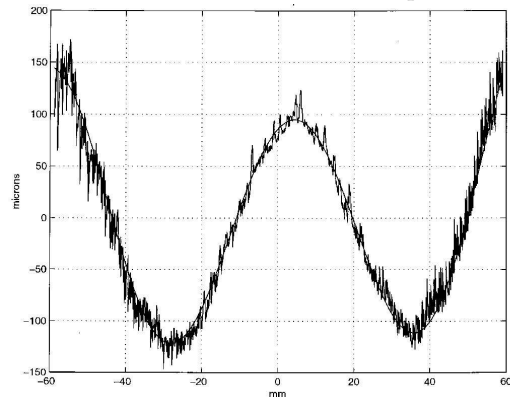


FIG. 2.— The residuals of the profile measurements of the free-standing plastically deformed reflector. The residuals have a characteristic polynomial shape. After fitting to a 8th order polynomial the surface roughness is found to be $8 \mu\text{m}$ RMS.

The membrane is a $50 \mu\text{m}$ rolled stainless steel foil with fabricated surface finish of $\sim 8 \mu\text{m}$ RMS. This is the same value measured after the surface measurements were fit to a parabolic + 8th order polynomial. The reflector as constructed is suitable for use in the far-infrared/submillimeter: the small scale surface roughness having a value of $\sim \lambda/25$, and the global wavefront error of $\sim \pm 1\lambda$ is correctable as outlined below. Copper, silver, and nickel membranes have also been used and give similar results.

5. SECONDARY AND TERTIARY REFLECTORS

In the case of a parabolic primary it is well known that an elliptical (Gregorian) or hyperbolic (Cassegrain) secondary results in a telescope system with an improved field-of-view. Even better performance can be achieved by adjusting the conic constants of the primary and secondary so that the Abbe sine condition is minimally violated. This conic approximation is the basis of the Ritchey-Chretien

solution. Schwarzschild (1905) solved the problem of finding the analytic form of the surfaces that exactly satisfy the sine condition. In the following sections algorithms are given that generate the shapes needed for corrective secondary and tertiary reflectors.

5.1. One Reflector Correction

A solution to the problem of correcting a spherical reflector with a single secondary is given by Head (1957) and Geruni (1964). The results are generalizable to non-spherical primary reflectors. Since only the secondary is adjustable the field-of-view of this system is smaller than that of either the classical Gregorian or the Ritchey-Chretien.

5.2. Two Reflector Correction

An aplanatic system is free of both astigmatism and coma, and has the widest focal surface of any design. An algorithm to generate aplanatic surfaces is described by Lundberg (1964). This algorithm can be generalized to generate corrective secondary and tertiary reflectors with a given primary reflector. Two conditions on the ray paths through the system are (Figure 3): 1) the Abbe sine condition

$$\frac{h}{\sin(\theta)} = k = |x_2 - x_1| + |x_2 - x_3| + ((x_3 - x_4)^2 + y_4^2)^{1/2};$$

2) constant path lengths for each ray from the entrance aperture to the focal point

$$l = k + |x_0 - x_1|.$$

The surfaces $M2(x)$ and $M3(x)$ are generated recursively by tracing rays through the system. The rays hit $M1$ and are deflected towards $M2$ and $M3$; $M2$ is adjusted so that the path length condition is satisfied while $M3$ is adjusted so that the sine condition is met. A visualization is provided by considering individual rays as strings of constant length. Where they contact a reflective surface the angles must satisfy the reflection law. With this procedure $M2(x)$ and $M3(x)$ are generated.

The best performance is obtained when tertiary $M3$ is located near the image of the primary produced by $M2$. This location is ideal for correcting the shape imperfections of the primary reflector. This can be seen by noting that a region on the primary is imaged to a region on the tertiary via the secondary reflector. Thus, by distorting the tertiary opposite to the shape imperfection of the primary a corrective system is produced. This applies to all

scales of spatial imperfections, with the large scales being the easiest to correct.

5.3. Tertiary Scanning

A complementary use for the tertiary is to allow fast scanning or tracking of an observation point by rotating the tertiary about an axis orthogonal to the optical axis. Since the tertiary is located at an image of the primary, this is optically equivalent to rotating the primary. Rotation of the tertiary effects a change in the observing direction without changing the illumination of the primary reflector. The tertiary is smaller than the primary, so the scanning or tracking is accomplished with high performance.

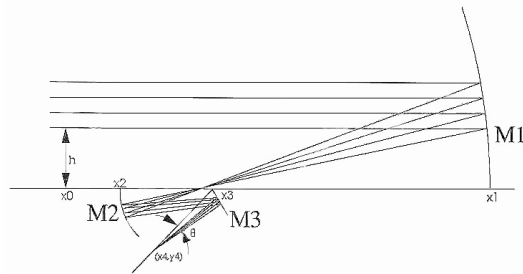


FIG. 3.— The 2 reflector corrector system ($M2$, $M3$) generated using a modified Lundberg algorithm. $M2(x)$ and $M3(x)$ are adjusted so that the conditions of constant path length and the Abbe sine condition are met. In a complementary use, $M3$ may be rotated to effect scanning on the sky.

6. SUMMARY AND CONCLUSIONS

This letter describes arrangements of reflectors that concentrate electromagnetic radiation with the primary reflecting surface formed by either stretching or tensioning a membrane over a suitable boundary. The systems are constructed so that the resulting telescopes have very low areal mass density ($\sim 1\text{kg/m}^2$) and are scalable to large apertures with diffraction limited performance.

I wish to thank my CARA, JPL, NSF, and STACEE colleagues for their criticisms and suggestions. Former students B. Crone and R. Leheany assisted in the initial stages of this work; G.H. Marion and A.K. George assisted with the construction and characterization of the plastically deformed reflector. This work was supported by NSF, the McDonnell foundation, NASA, and the Fullahm award of the Dudley observatory.

REFERENCES

- Almgren, F.J. 1969 *Plateau's Problem*. Benjamin.
 Bateman, H. 1932 *Partial Differential Equations of Mathematical Physics*. Cambridge.
 Cardona-Nunez, O. et al. 1987 *Applied optics* **26**, 4832.
 Claydon, B. 1975 *Marconi Review* **1st quarter**, pp 14-43.
 Dragone, C. 1982 *IEEE Trans. Ant. Prop.* **AP-30**, 331.
 Geruni, P.M 1964 *Radiotechnica i Electronika* (Eng. trans.), **9**, 1.
 Gregory, J. 1663, *Optica Promota* .
 Head, A.K 1957 *Nature*, **179**, 692.
 Isenberg, C. 1992 *The Science of Soap Films and Soap Bubbles*. Dover.
 King, H.C. 1979 *The History of the Telescope*. Dover.
 Lundberg, R.K. *Mathematical Theory of Optics*. University of California Press, 1964 (p208).
 Newton, I. 1672 *Phil. Trans.*, **7**, pp 4004-10.
 Murphy, L.M. 1987 *Journal of Solar Energy Engineering* **109**, 111-120
 Schroeder, D.J. 1987 *Astronomical Optics*. Academic Press.
 Schwarzschild, K. 1905 *Astr. Mitteilungen Kognigl. Sternwarte Gottingen*, **10**,1.
 Stewart, D. 1965 *Proc. Instn. Mech. Engrs.* **180**, 371.
 Struik, D.J. 1961 *Lectures on Classical Differential Geometry*. Addison-Wesley.
 Weil, N.A. and Newmark, N.M. 1955 *Journal of Applied Mechanics*, Dec.,pp 533-538.